Optimizing Capacity-Expansion Planning of Groundwater Supply System between Cost and Subsidence

Hone-Jay Chu[1] and Liang-Cheng Chang[2]

Abstract: This work solves an optimal capacity-expansion planning problem with land subsidence constraints using a hybrid algorithm that combines the genetic algorithm (GA) and constrained differential dynamic programming (CDDP). The main structure of the hybrid algorithm is the GA, in which each chromosome represents a possible network design and its expansion schedule. The present fixed cost of each chromosome is computed easily using the GA, and CDDP is then used to solve the optimal pumping rates and compute the optimal present operating costs associated with the chromosome. Simulation results indicate that the well network has lower total present cost with the capacity-expansion system instead of installing the full system capacity at the beginning. However, the well network designed by the capacity-expansion model without considering land subsidence may induce more local land subsidence than that determined by the conventional model demonstrating the necessity of considering land subsidence constraints in the system design. This work also investigates other important issues related to the optimal design of the system-installing schedule. The proposed model is highly promising for facilitating a cost-efficient well system design for regional groundwater supply and environmental conservation.

DOI: 10.1061/(ASCE)HE.1943-5584.0000219

CE Database subject headings: Land subsidence; Algorithms; Computer programming; Groundwater supply; Costs.

Author keywords: Land subsidence; Genetic algorithm; Constrained differential dynamic programming; Groundwater supply.

Downloaded from ascelibrary.org by National Chiao Tung University on 04/24/14. Copyright ASCE. For personal use only; all rights reserved.

Introduction

Expanding water resource system capacity is a cost-effective strategy that satisfies increasing water demand (Jenkins et al. 2004; Pulido-Velazquez et al. 2006; Chang et al. 2009) for increasing populations and rising economics. Groundwater plays a vital role in regional water resources and is used in numerous ways such as for domestic, agricultural, and industrial purposes. Optimizing groundwater capacity expansion becomes a significant issue in water resources management. Basagaoglu and Yazicigil (1994) developed a groundwater management model in a hypothetical multilayer confined aquifer with capacity expansion to determine optimal expansion schedules and time-varying pumping rates. The models included the system response using the response matrix method. The study used three approximation methods to simplify this capacity-expansion problem. Watkins and McKinney (1998) developed a capacity-expansion model for conjunctive use of surface and subsurface water. The study applied two decomposition methods, the generalized Benders decomposition (GBD) and outer approximation (OA), to restructure the original mixed integer nonlinear programming (MINLP) problem to a finite alternative sequence of mixed integer linear programming (MILP) master problems, and nonlinear programming (NLP) subproblems. Their research focused on the problem with confined aquifer and constant pumping rates because of linear and nondynamic approximation. Voivontas et al. (2003) used the nonlinear generalized reduced gradient method to solve the problem of groundwater supply capacity expansion for small islands. The study considered only the total pumping capacity and not the pumping network design.

Groundwater overdraft causes land subsidence problems in many places (Ortega-Guerrero et al. 1993; Sun et al. 1999; Chen et al. 2003); therefore considering potential consequences of land subsidence due to groundwater withdrawal is important (Adrian et al. 1999; Don et al. 2006). Pumping restrictions have resulted from severe land subsidence due to aquitard consolidation caused by aquifer exploitation. Pumping decreases water pressure and increases the solid matrix effective stress. Solid skeleton compaction in the aquifer causes soil displacement. Land subsidence refers to the deformation of a two-phase medium consisting of pore fluid and deformation porous media. Biot (1941) regarded land subsidence as a three-dimensional phenomenon in which the flow of water and the strain in the solid matrix are interrelated through Terzaghi's concept of effective stress. Some researchers simplified the process to obtain land subsidence. Jacob (1940) assumed that only vertical displacement takes place and that all stresses act only in a vertical direction. As a result, porosity becomes a water pressure function. The soil velocity effect is neglected in determining the water pressure distribution. Water pressure is then subsequently used to determine vertical land subsidence. Verruijt (1969) employed Biot's theory, accounting for the soil velocity effect on groundwater flow but assumed vertical displacement only, thereby simplifying Biot's theory into a two-step approach. The two-step approach obtained the hydraulic head based on mass conservation first, and then used the result to determine the vertical soil displacement.

[1]Postdoctoral Fellow, Dept. of Bioenvironmental Systems Engineering, National Taiwan Univ., No. 1, Sec. 4, Roosevelt Rd., Taipei 10617, Taiwan. E-mail: honejaychu@gmail.com

[2]Professor, Dept. of Civil Engineering, National Chiao Tung Univ., 1001 Ta Hsueh Rd., Hsinchu 30050, Taiwan (corresponding author). E-mail: lcchang31938@gmail.com

Note. This manuscript was submitted on August 6, 2008; approved on December 14, 2009; published online on December 17, 2009. Discussion period open until January 1, 2011; separate discussions must be submitted for individual papers. This paper is part of the ***Journal of Hydrologic Engineering***, Vol. 15, No. 8, August 1, 2010. ©ASCE, ISSN 1084-0699/2010/8-632–641/$25.00.

Few groundwater management models consider land subsidence constraints from the environmental perspective. Larson et al. (2001) found that inelastic soil compaction causes large amounts of land subsidence. The study determined maximum groundwater withdraws of each subbasin without causing land subsidence and limited groundwater withdraw by constraints of water table drawdown. Liu and Helm (2008) presented the inverse aquifer compaction model for identifying parameters that control land subsidence caused by groundwater withdrawal. The results demonstrated that the proposed model can be applied to a real field case. Chang et al. (2007b) considered the deterministic and stochastic management model in a confined aquifer considering land subsidence, but used the response matrix approach as a groundwater flow simulation model and a one-dimensional consolidation equation to estimate land subsidence.

Therefore, a cost-effective and environmentally friendly strategy for groundwater system planning increases the system capacity step by step based on the water demand increase and considers land subsidence constraints simultaneously. However, the problem is complex, nonlinear, dynamic, and discrete. The dynamic nature of the problem is similar to other groundwater management problems and can greatly increase computational loading when problem time steps increase. Several researches proposed a dynamic algorithm (CDDP) to reduce the computational requirement (Jones et al. 1987; Chang et al. 1992; Culver and Shoemaker 1992, 1993; Mansfield and Shoemaker 1999). The GA can be used efficiently to solve mixed-integer programming groundwater management problems (McKinney and Lin 1994; Huang and Mayer 1997). Hsiao and Chang (2002) integrated the genetic algorithm (GA) and constrained differential dynamic programming (CDDP) to solve a groundwater management problem that considers fixed and operation costs simultaneously. The study dealt with the nonlinear, dynamic, and discrete optimization problems in groundwater management without considering capacity expansion and land subsidence constraints.

This study proposes a novel procedure to solve a groundwater optimal planning problem considering both capacity expansion and land subsidence constraints. The main algorithm structure integrates the GA and CDDP adapted from the study of Hsiao and Chang (2002). However, the proposed algorithm requires modification to accommodate the capacity expansion of the groundwater supply system and land subsidence constraints. The proposed algorithm reduces the computational loading caused by time-varying pumping rates (Murray and Yakowitz 1979; Jones et al. 1987; Hsiao and Chang 2002) as well as accommodates the discrete combinatorial problem induced by well network expansion. Simulation results demonstrate the proposed model capability to obtain an optimal stepwise-expansion network design and also show that the capacity-expansion policy indeed reduces present total cost value but increases land subsidence. This is an example of the trade-off between developing cost and environmental protection. This study not only proposes a novel hybrid model for solving an optimal groundwater network design problem concerned with both developing cost and environmental impact, but also reveals important groundwater development issues. The results are valuable references for sustainable groundwater management.

Formulation of Groundwater Management Model

The proposed model seeks to minimize the total water supply system cost for an unconfined aquifer and the design policy expands the stepwise groundwater network capacity. The total cost includes both fixed costs of well installation and operating costs of time-varying pumping. The optimization model can be formulated as below:

Objective function:

$$\min_{\{I,u_{t,i}\}} z = \sum_{i\in I}\left\{ c_1 y_i \frac{1}{(1+r)^{n(P_i-1)}} + \sum_{t=1}^{T}\left[c_2 u_{t,i}(L_i - h_{t+1,i})\frac{1}{(1+r)^t}\right]\right\}, \quad I\subset\Omega \tag{1}$$

subject to

$$\{x_{t+1}\} = T(x_t, u_t, t), \quad t=1,2,\ldots,T \tag{2}$$

$$s_{T,k} \le s_{\max}, \quad k\in K \tag{3}$$

$$h_{t,k} \ge h_{\min}, \quad k\in K \tag{4}$$

$$\sum_{i\in I} u_{t,i} \ge d_t, \quad t=1,2,\ldots,T; \quad i\in I \tag{5}$$

$$u_{\min} \le u_{t,i} \le u_{\max}, \quad t=1,2,\ldots,T; \quad i\in I \tag{6}$$

where I=set of well locations for a candidate network design and the subset of Ω; Ω=set of all potential well sites for installed wells; K=set of observation wells; and i=ith well in a candidate network design I. k=kth well in observation network K; t=tth operation time step; y_i=depth of the ith well in a candidate network design; P_i=construction period of the ith well and each construction period contains n operation time steps ($n\ge 1$); r =interest rate; $u_{t,i}$=decision variable (time-varying pumping rate) for the ith well in a candidate network at the tth operation time step; L_i=ground surface elevation for the ith well in a candidate network design; and h_{t+1}=hydraulic head at $(t+1)$-th time step. $s_{T,k}$=land subsidence for the kth well in the observation at Tth time step; $s_{\max}$=maximum allowable amount of land subsidence; $h_{\min}$=minimum allowable amount of hydraulic head; d_t=amount of water demand at operation time step t; c_1=well installation cost per unit well depth; c_2=pumping cost per unit volume of water formulated as $c_2=r\times c_3\times\Delta t$; r=unit weight; c_3=electric power cost per unit work for pumping groundwater; Δt=time interval of each time step; $u_{\max}$=maximum pumping rate; and $u_{\min}$=minimum pumping rate.

Eq. (1) represents the present total cost value. The first term in the right hand side of Eq. (1) is the present fixed cost value and the second is the present operation cost value. The decision variable is $u_{t,i}$ and is the pumping rate for the ith well in the candidate network at the operation time step t. Eq. (2) is the transfer function $T(x_t,u_t,t)$ of state variables. $x_t=[h_t:s_t]^T$=continuous state variables representing hydraulic heads (h_t) and land subsidence (s_t); u_t represents the control vector. Eq. (3) limits the land subsidence to the maximum allowable land subsidence. Eq. (4) limits the hydraulic head to the minimum allowable hydraulic head. In site application, the allowable hydraulic head is set as the preconsolidation head to prohibit the inelastic compaction (Larson et al. 2001). Eq. (5) requires the total pumping volume to fulfill the water demand. Eq. (6) is the capacity constraint for each well. The hydraulic head at time step $t+1$ (h_{t+1}) is described as follows:

J. Hydrol. Eng. 2010.15:632-641.

Downloaded from ascelibrary.org by National Chiao Tung University on 04/24/14. Copyright ASCE. For personal use only; all rights reserved.

$$\{h_{t+1}\} = \left([A(h_{t+1})] + \frac{[B]}{\Delta t}\right)^{-1}\left(\frac{[B]}{\Delta t}\{h_t\} - \{F_h\} + [L_h]\{u_t\}\right), \quad t = 1,2,\ldots,T \quad \forall \quad I \tag{7}$$

where the coefficients of matrices and vectors derive from the finite-element method (FEM) flow model (Chang et al. 1992; Hsiao and Chang 2002).

The land subsidence at time step $t+1$ (s_{t+1}) follows the approach that develops a simplified version of Biot's approach based on the assumption that soil displacements occur only in the vertical direction (Bear and Verruijt 1987). This assumption decouples problem solving for the pore-water pressure and solid matrix deformation. The solutions are computed in two steps: computing the pore-water pressure first and then calculating land subsidence by the relationship between the soil strain and pore-water pressure change. The one-dimensional consolidation is expressed as

$$\Delta s_{t,i} = \int_B \varepsilon_b(x,y,z,t)dz = \int_B \frac{p^e(x,y,z,t)}{(\lambda + \mu)}dz \tag{8}$$

where $\Delta s_{t,i}$ represents the land subsidence increment at location i and time step t; where x and y=horizontal coordinate; ε_b =volumetric soil strain; p^e denotes excess pore-water pressure; λ and μ denote Lame's coefficients representing the elastic coefficient; and B denotes the layer thickness. The study furthermore assumes a horizontal flow, and p^e is elevation independent. Neglecting the swell due to increased pore-water pressure, Eq. (8) can be simplified as Eq. (9) (Chang et al. 2007b)

$$\Delta s_{t,i} = -\frac{\rho g(h_{t+1,i} - h_{t,i})}{\lambda + \mu}B \quad \text{for} \quad h_{t+1,i} < h_{t,i}$$

$$=0, \quad \text{otherwise} \tag{9}$$

The land subsidence at time step $t+1$ is then computed as

$$\{s_{t+1}\} = \{s_t\} + \{\Delta s_t\}, \quad t = 1,2,\ldots,T \tag{10}$$

Reformulation of the Problem

The problem defined by Eqs. (1)–(6) is solved by a novel hybrid algorithm modified from Hsiao and Chang (2002, 2005). This study explores the problem structure and reformulates the problem into a two-level optimization problem to facilitate hybrid algorithm development and ensure that the hybrid algorithm consistently solves the problem.

Main problem

$$\min_{\{I\}} z = \sum_{i \in I}\left(c_1 y_i \frac{1}{(1+r)^{n(P_i-1)}}\right) + J^*(I), \quad I \subset \Omega \tag{11}$$

Subproblem (for each network alternative design, I)

$$J^*(I) = \min_{u_{t,i}} \sum_{i \in I}\sum_{t=1}^{T} c_2 u_{t,i}(L_i - h_{t+1,i})\frac{1}{(1+r)^t} \tag{12}$$

subject to

$$\text{Eqs. (2), (3), (4), (5), (6)} \tag{13}$$

Solving the two-level optimization problem defined by Eqs. (11)–(13) is equivalent to solving the original one defined by Eqs. (1)–(6). The main problem [Eq. (11)] contains all the discrete variables: fixed cost and discrete decision variables, and stepwise-expansion network designs. This study uses the GA to solve the main problem. The GA accomplishes the discrete nature of searching for optimal well location network alternatives. Within the GA, each chromosome (stepwise-expansion network design) associates a subproblem and the subproblem solution is the optimal operating cost. The subproblem [Eqs. (12) and (13)] contains nonlinear and dynamic characteristics. The CDDP enables a significant reduction in the "working" dimensionality of the algorithm over that of mathematical programming algorithms by taking advantage of the dynamic nature of groundwater supply and water quality optimization problems through stagewise decomposition (Murray and Yakowitz 1979; Jones et al. 1987; Hsiao and Chang 2002). Hence, the CDDP algorithm, a nonlinear dynamic algorithm, is suitable to solve the subproblem.

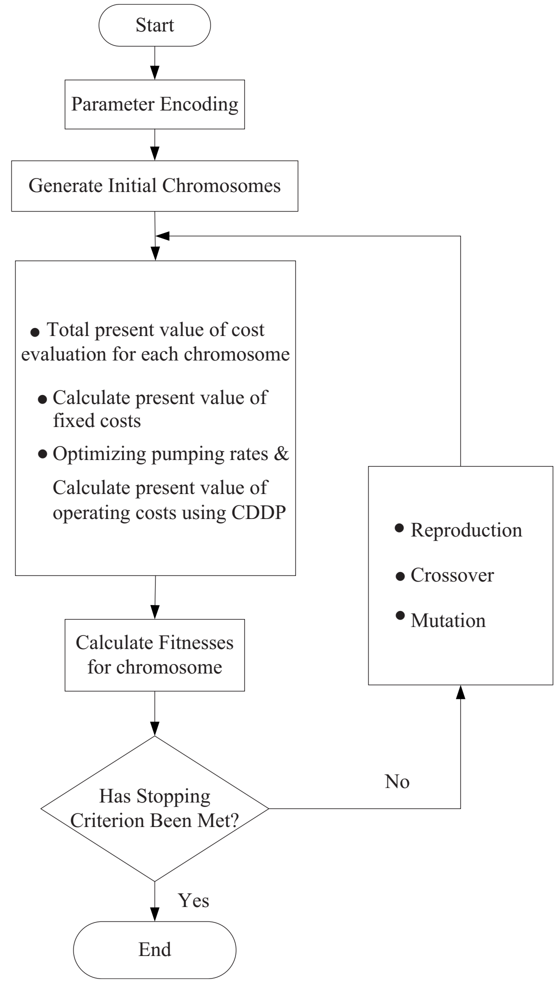

Fig. 1. Flowchart for the groundwater management model

Algorithm to Solve the Groundwater Management Problem

This study develops a hybrid algorithm by integrating the GA and modified CDDP as illustrated in Fig. 1 to solve the two-level formulation described in Eqs. (11)–(13). The hybrid algorithm in Fig. 1 includes two parts: GA iteration and CDDP. The GA accomplishes the discrete search for an optimal stepwise-expansion network design. The modified CDDP algorithm during the GA

J. Hydrol. Eng. 2010.15:632-641.

Downloaded from ascelibrary.org by National Chiao Tung University on 04/24/14. Copyright ASCE. For personal use only; all rights reserved.

Table 1. Example of Chromosome Coding for Stepwise-Expansion Network Design

Number of candidate site	1	2	3	4	5	....	21
Chromosome	00	01	00	11	10	....	01
Decimalization value	0	1	0	3	2	....	1
State of the candidate site	Not installing well	Installing well at beginning of Period I	Not installing well	Installing well at beginning of Period III	Installing well at beginning of Period II	....	Installing well at beginning of Period I

search is used to determine optimal present value of operation cost and optimal time-varying pumping rates for each well in the network design. The CDDP algorithm developed in this study is modified from that proposed by Hsiao and Chang (2002), with the addition of the transition equation and the derivative of that in land subsidence (s_t). Consequently, the derivative of the transition equation with respect to x_t and u_t is modified as

$$\left[\frac{\partial T}{\partial x_t}\right] = \left[\frac{\partial x_{t+1}}{\partial x_t}\right] = \begin{bmatrix} \frac{\partial h_{t+1}}{\partial h_t} & \frac{\partial h_{t+1}}{\partial s_t} \\ \frac{\partial s_{t+1}}{\partial h_t} & \frac{\partial s_{t+1}}{\partial s_t} \end{bmatrix} \tag{14}$$

$$\left[\frac{\partial T}{\partial u_t}\right] = \left[\frac{\partial x_{t+1}}{\partial u_t}\right] = \begin{bmatrix} \frac{\partial h_{t+1}}{\partial u_t} \\ \frac{\partial s_{t+1}}{\partial u_t} \end{bmatrix} \tag{15}$$

The main structure of the hybrid algorithm, as indicated in Fig. 1, is a simple GA embedded in a modified CDDP algorithm (Chang and Hsiao 2002; Hsiao and Chang 2002, 2005; Chu et al. 2005; Chang et al. 2007a). The chromosome (stepwise-expansion network design) population must be generated in the beginning of the GA iteration. Besides the CDDP, the main loop includes reproduction, crossover, mutation, and computing the fitness of each chromosome represented by the total cost of each network design. The whole algorithm solves the main problem defined by Eq. (11) and the CDDP solves the subproblem defined by Eq. (12) associated with each chromosome.

The modifications of the GA and CDDP for the capacity expansion are described in the following. The details of the stepwise-expansion network design by the GA could refer to Chang et al. (2009). This study assumes three expansion periods for the pumping network and includes four options for each candidate well site: (1) the noninstalled well; (2) the installed well at the beginning of Period I; (3) the installed well at the beginning of Period II; and (4) the installed well at the beginning of Period III. Hence, a candidate well site requires more than a binary bit to represent the well installation status and this study uses two binary bits for that. Since each candidate site is associated with two binary bits in a chromosome, the number of bits for a chromosome is twice the total number of candidate well sites. Table 1 presents an example to illustrate the chromosome-coding scheme in the GA and each chromosome represents a stepwise-expansion network design. The example shows that each two-bit binary is decimalized into 0 to 3. A binary string composed of binary bits represents the chromosome. A decimalized value equaling 0 indicates no well will be installed at the associated candidate site. A decimalized value equaling 1 represents a well to be installed at the associated candidate site in the beginning of Period I. Similarly, a decimalized value equaling 2 or 3 means a well will be installed at the associated candidate site in the beginning of Period II or III. Therefore, Candidate Well Sites 1 and 3 in the example did not install well, while Candidate Well Sites 2, 4, and 5 installed well at the beginning of Period I, Period III, and Period II, respectively (Table 1). Based on the above, each candidate well will require more binary bits to represent the well installation status if the number of network expansion periods increase. Moreover, the CDDP algorithm modification is necessary when considering the capacity expansion. The dimension of pumping rates changes with the period since the pumping rates of each well are the decision variables. The pumping wells are installed at the beginning of each period for a stepwise-expansion network. As the network designs (chromosomes) have defined the number of wells at each period, the decision variable dimension of the CDDP is determined.

The GA algorithm involves three major operators—the reproduction operator, the crossover operator, and the mutation operator (McKinney and Lin 1994; Hsiao and Chang 2002). If the model has not met the stopping criteria, then the parent generation undergoes reproduction, crossover, and mutation generating the next generation of offspring. In the study, the set of GA parameters including the population size, crossover probability, and mutation probability were determined by the sensitivity analysis of the GA's parameters (Goldberg 1989; Hsiao and Chang 2002). In all of the cases, the population size, crossover probability, and mutation probability were 100, 0.8, and 0.01, respectively. In addition, reproduction is implemented in this study by using the roulette wheel approach. A detailed discussion of the GA could refer to McKinney and Lin (1994), Morshed and Kaluarachchi (2000), Chang and Hsiao (2002), Hsiao and Chang (2002), and Bayer and Finkel (2004).

Results and Discussion

Rapidly increasing CPU time is caused by a large number of state variables in the CDDP algorithm (Mansfield et al. 1998; Chu and Chang 2009). Consequently, numerical analyses on a hypothetical groundwater supply problem were performed to verify the effectiveness of the proposed methodology. The groundwater supply problem is adapted from the example of Hsiao and Chang (2002). Fig. 2 displays the aquifer which is assumed to be homogeneous and isotropic. The $3{,}000\ \text{m} \times 5{,}000\ \text{m}$ site incorporates 77 finite-element nodes, 60 elements, and 35 potential well locations. Constant-head and no-flow boundaries circumvent the flow domain. The initial condition of the hydraulic head distribution prior to pumping is assumed to be steady state. Furthermore, the aquifer properties and simulation parameters are listed in Table 2. The initial conditions on the hydraulic head are $h_0=80$ m and the thickness of the aquifer (L) is 100 m. In the management model, the planning horizon is 15 years and is divided into three management periods. There are 60 time steps and each time step (Δt) is 0.25 year. The two Lame constants λ and μ are the elastic coefficients, which are determined experimentally for a given porous matrix (Bear and Verruijt 1987; Chang et al. 2007b). The two

Downloaded from ascelibrary.org by National Chiao Tung University on 04/24/14. Copyright ASCE. For personal use only; all rights reserved.

J. Hydrol. Eng. 2010.15:632-641.

Downloaded from ascelibrary.org by National Chiao Tung University on 04/24/14. Copyright ASCE. For personal use only; all rights reserved.

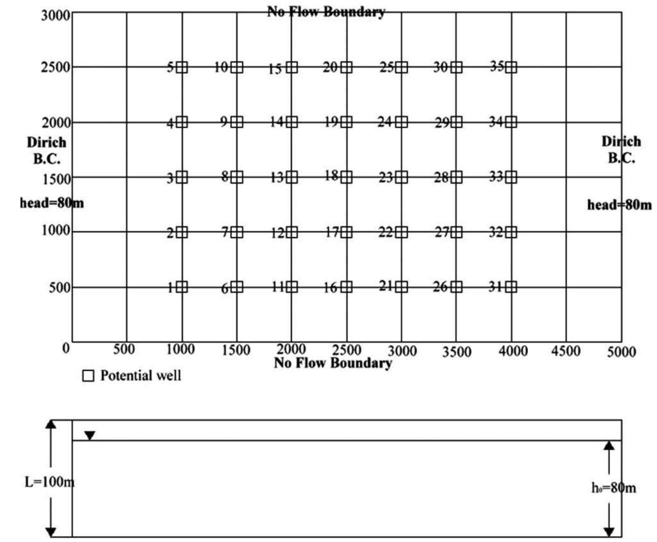

Fig. 2. Hypothetical aquifer in the study

Table 2. Aquifer Properties and Simulation Parameters of Each Case

Parameter	Value
Aquifer thickness	100 (m)
Initial hydraulic head	80 (m)
Planning horizon	15 (year)
Simulation time step	0.25 (year)
Horizontal hydraulic conductivity	0.001 m/s
Vertical hydraulic conductivity	0.001 m/s
Porosity	0.2
Specific yield	0.1
Lame's coefficients	$\mu = 6 \times 10^8$ N/m^2 $\lambda = 10^9$ N/m^2
Annual interest rate	8%
Cost of unit length well installation	\$200
Cost per kilowatt-hour	\$0.45

parameters in the study are followed by Chang et al. (2007b). Table 3 summarizes the basic assumptions of all the cases, which include the management model type, water demand curve, total amount of water demand, and maximum allowable land subsidence. The three time-increasing water demand curves include the linear curve, concave curve, and convex curve (Basagaoglu and Yazicigil 1994) (Fig. 3). Moreover, the maximum allowable land subsidence of Cases 2–6 is 0.40 m and that of Case 7 is at 0.30 m. The minimum allowable hydraulic heads at all cases are 50 m.

Impact of with or without Capacity-Expansion on Present Total Cost and Land Subsidence

Cases 1 and 2 examine the impact of with or without considering capacity expansion on the optimal present total cost and land subsidence. The total cost present value includes present values of the operation cost and fixed cost. The same demand curve (convex curve) and annual interest rate are applied for the two cases. Both cases have a total of 60 time steps. The construction policy in Case 1 cannot accommodate the expanding management model and is only concerned with the well system installation at the start of the planning period. Case 2 considers capacity expansion and its well system capacity expands at the beginning of the first, sixth, and 11th year. The planning model proposed in this study computes wells to be installed at the expanding time.

Table 4 indicates that the optimal construction policy for Case 1 installs the required 22 wells in the beginning, while the optimal network expanding schedule for Case 2 installs eight wells at the beginning of the first period; then expands to 11 wells at the beginning of the second period; and finally expands to 22 wells at the beginning of the last period. Although the total well numbers at the end are the same for the two cases, Case 1 installs all the required wells in the beginning to fulfill the water demand at the end, while Case 2 expands its well system according to increasing water demand. Fig. 4 shows the time-varying pumping rates per well in Cases 1 and 2. The different system construction policy

Table 3. Case Definitions

	Management model type	Water demand curve	Total water demand (10^6 m^3)	Maximum allowable subsidence (m)
Case 1	Without capacity expansion	Convex curve	9.1	NA
Case 2	With capacity expansion	Convex curve	9.1	0.4
Case 3	With capacity expansion	Convex curve	8.6	0.4
Case 4	With capacity expansion	Convex curve	8.1	0.4
Case 5	With capacity expansion	Linear curve	9.1	0.4
Case 6	With capacity expansion	Concave curve	9.1	0.4
Case 7	With capacity expansion and active land subsidence constraints	Convex curve	9.1	0.3

Note: NA = not available.

Table 4. Optimal Pumping and Construction Policy under Different Water Demands (Cases 1–4)

Total water demand (10^6 m^3)	9.1				8.6			8.1		
Case number	Case 1	Case 2			Case 3			Case 4		
Construction period number	I	I	II	III	I	II	III	I	II	III
Well numbers for each period	22	5	11	22	5	11	20	5	10	19
Present fixed cost value	440,000	280,392			262,277			248,817		
Present operation cost value	992,484	993,006			945,080			880,677		
Present total cost value	1,432,484	1,273,398			1,207,357			1,129,494		

J. Hydrol. Eng. 2010.15:632-641.

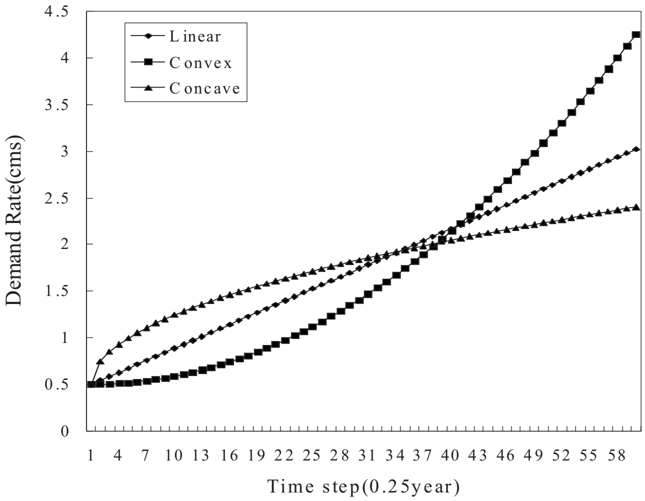

Fig. 3. Various water demand curves

causes great savings of the fixed cost present value for Case 2 by comparing the fixed cost of the two Cases in Table 4 and Fig. 5(a). Considering the time value of money, the capacity-expansion model has a lower total cost present value than that installs full system capacity initially.

The fixed cost savings may induce the controversy effect of increasing land subsidence by comparing the land subsidence contour map in Figs. 6(a and b). Figs. 6(a and b) indicate more

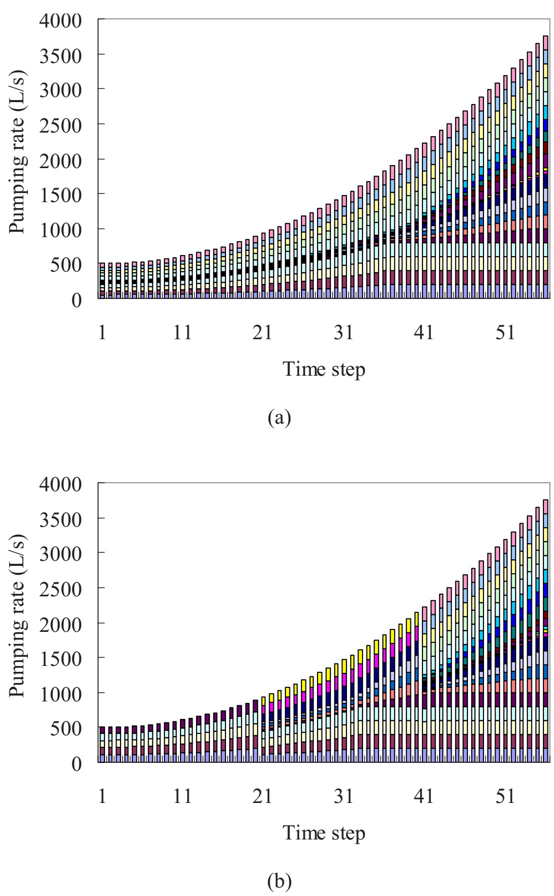

Fig. 4. Time-varying pumping rates per well with and without considering capacity expansion: (a) Case 1; (b) Case 2

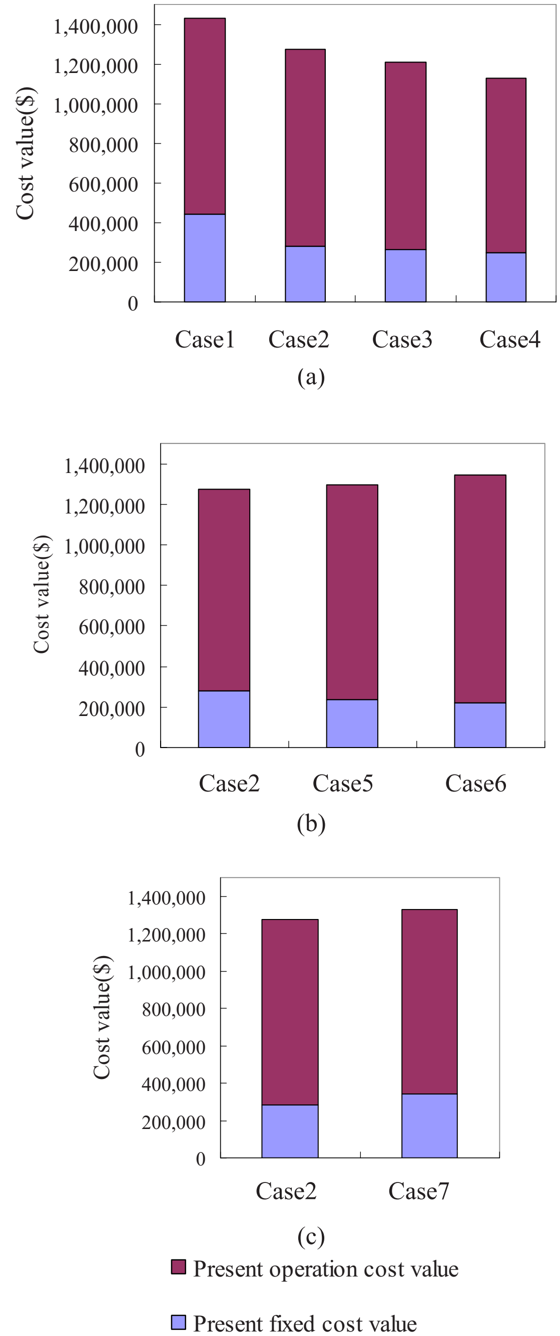

Fig. 5. Present value of the costs in the cases: (a) Cases 1–4; (b) Cases 2, 5, and 6; and (c) Cases 2 and 7

land subsidence for Case 2 [Fig. 6(b)] than Case 1 [Fig. 6(a)]. The increased land subsidence may be caused by increased pumping rates per well. The number of wells for Case 2 at the first and second periods are only 5 and 11 wells; therefore, the pumping rates per well for Case 2 are much more than Case 1, since both cases must have the same total pumping rates to fulfill the same water demand (Fig. 4). The result shows that the optimal system design using the capacity expending model is more cost-effective, but may have higher land subsidence risk. This finding demonstrates the necessity of considering land subsidence constraints in system design.

J. Hydrol. Eng. 2010.15:632-641.

Downloaded from ascelibrary.org by National Chiao Tung University on 04/24/14. Copyright ASCE. For personal use only; all rights reserved.

Downloaded from ascelibrary.org by National Chiao Tung University on 04/24/14. Copyright ASCE. For personal use only; all rights reserved.

Impact of Total Water Demand on Present Total Cost and Land Subsidence

Cases 2, 3, and 4 examine the impact of the total water demand on the present total cost and land subsidence. The demand curves are all convex and the total water demand in 15 years varies from 8.1 to 9.1 (10^6 m^3).

This study finds an optimal pumping and construction policy to satisfy these demands. The present total cost for each case is shown in Table 4 and Fig. 5(a). Results show that the amount of present total cost, including fixed and operating costs, increases with water demand, i.e., the present total costs are Case 2 >Case 3>Case 4. Besides cost, Figs. 6(b–d) show the land subsidence in Cases 2–4, respectively. The results indicate that the maximum land subsidence value also increases with total demand. Therefore, groundwater pumping must consider land subsidence to avoid the potential environmental impact.

Impact of Water Demand Curve on Present Total Cost and Land Subsidence

Cases 2, 5, and 6 are designed to investigate the impact of the water demand curve on costs and land subsidence. The three cases have the same total water demand over 15 years but with distinct water demand curves in time. The curves are convex, linear, and concave, respectively, as shown in Fig. 3.

Table 5 summarizes various present optimal policy costs for the three cases. The fixed cost is a function of the number of wells. As indicated in Fig. 3, Case 2 with the convex water demand curve has the largest water demand, while Case 6 with the concave water demand curve has the smallest water demand, at the last time step. Since well numbers should be proportional to the water demand for an optimal policy, Case 2 has the maximum number of wells installed at the last expansion period, while Case 6 has the minimum number of wells installed at the last period, as shown in Table 5. Since well numbers for Case 2 are much larger than the other two cases, Case 2 has the largest present fixed cost. However, Case 2 has more water pumping than the other cases near the end of the planning period since the pumping rate is related to water demand. Nevertheless, computing the present operation cost value near the ending time has a more discounting effect. Therefore, Case 2 has the minimum present operation cost shown in the table and Fig. 5(b). Since the present operation cost dominates the present total cost, Case 2, with convex water demand, has the least present total cost [Fig. 5(b)].

Figs. 6(b, e, and f) show the land subsidence for various demand patterns indicated above. The land subsidence is largest at the end of a convex demand curve and smallest at the end of a concave demand curve. Since pumping rates are largest at the end for the convex demand curve, the result denotes that land subsidence is most serious when pumping rates are largest [Fig. 6(b)]. This work therefore suggests that land subsidence be considered when the demand increases sharply.

Impact of Land Subsidence Constraints on Present Total Cost and Land Subsidence

Cases 2 and 7 both consider capacity expansion and the same demand increasing curve but with different land subsidence constraints to investigate land subsidence limitations on the present total cost. The land subsidence constraint of Case 7 is tighter than that of Case 2 at 0.30 m (Case 7) and 0.40 m (Case 2), respectively.

Table 6 summarizes optimal solutions for Cases 2 and 7. The optimal construction policy of Case 2 indicates that the network system must install five wells initially, and then expand to 11 wells, and finally to 22 wells. The optimal construction policy of Case 7 installs the network with nine wells, 16 wells, and 23 wells in sequence. The total well numbers and present total cost for Case 7 is larger than that of Case 2 in which the present fixed cost of Case 7 is higher than that of Case 2, while the present operation cost of Case 7 is slightly lower than Case 2 [Fig. 5(c)]. According to Figs. 6(b and g), the maximum land subsidence of Case 2 is 0.35 m [Fig. 6(b)] and that of Case 7 is 0.28 m [Fig. 6(g)]. A reasonable result is that the present total cost increases when the environmental impact reduces.

Furthermore, the computational loading required for solving the optimal schedule design of a groundwater supply system may increase with the problem size significantly (Mansfield et al. 1998). The details of the computational loading in the model are also discussed in Chang et al. (2009). However, since the main computation algorithm is the GA, applying a parallel computation to model computing could be easily implemented to reduce the computational time.

Conclusion

This work solves an optimal capacity-expansion planning problem with land subsidence constraints using a novel hybrid algorithm that combines the GA and CDDP. This study explores mathematical characteristics of the problem and reformulates it as a two-level optimization problem in order to facilitate the GA and CDDP algorithm application. Based on the two-level formulation, discrete decision variables of the problem are solved in the main problem using the GA, while continuous decision variables of the problem are computed in the subproblem using CDDP. Numerical studies based on a homogeneous isotropic unconfined aquifer demonstrate the proposed novel model capability and reveal several important points. Investigating the total water demand impact on the present total cost of optimal design and land subsidence shows that the amount of present total cost, including fixed and operating costs, increases with the water demand, and land subsidence also increases with the total demand. By investigating the impact of the water demand curve on present costs of optimal design and land subsidence with the same total water demand shows that the water demand curves and discounting of monetary value have a joint effect on the present fixed cost, present operating cost, and present total cost. For instance, while the optimal design has the least present total cost for the convex demand curve, its land subsidence is the largest. By contrast, the present total cost for the concave demand curve is the most expensive and land subsidence is least. Results from the convex demand curve in this study denote that land subsidence is largest when demand increases sharply.

Research on the influence of land subsidence constraints on the present total cost of optimal design shows that the present total cost increases when allowable limitations of land subsidence are more serious. Examining optimal solutions obtained by with or without considering capacity expansion reveals that optimal system design using the capacity expanding model is more cost-effective but may have higher land subsidence risk. The study provides a way for balancing the trade-off between the cost reduction and environmental conservation.

J. Hydrol. Eng. 2010.15:632-641.

Downloaded from ascelibrary.org by National Chiao Tung University on 04/24/14. Copyright ASCE. For personal use only; all rights reserved.

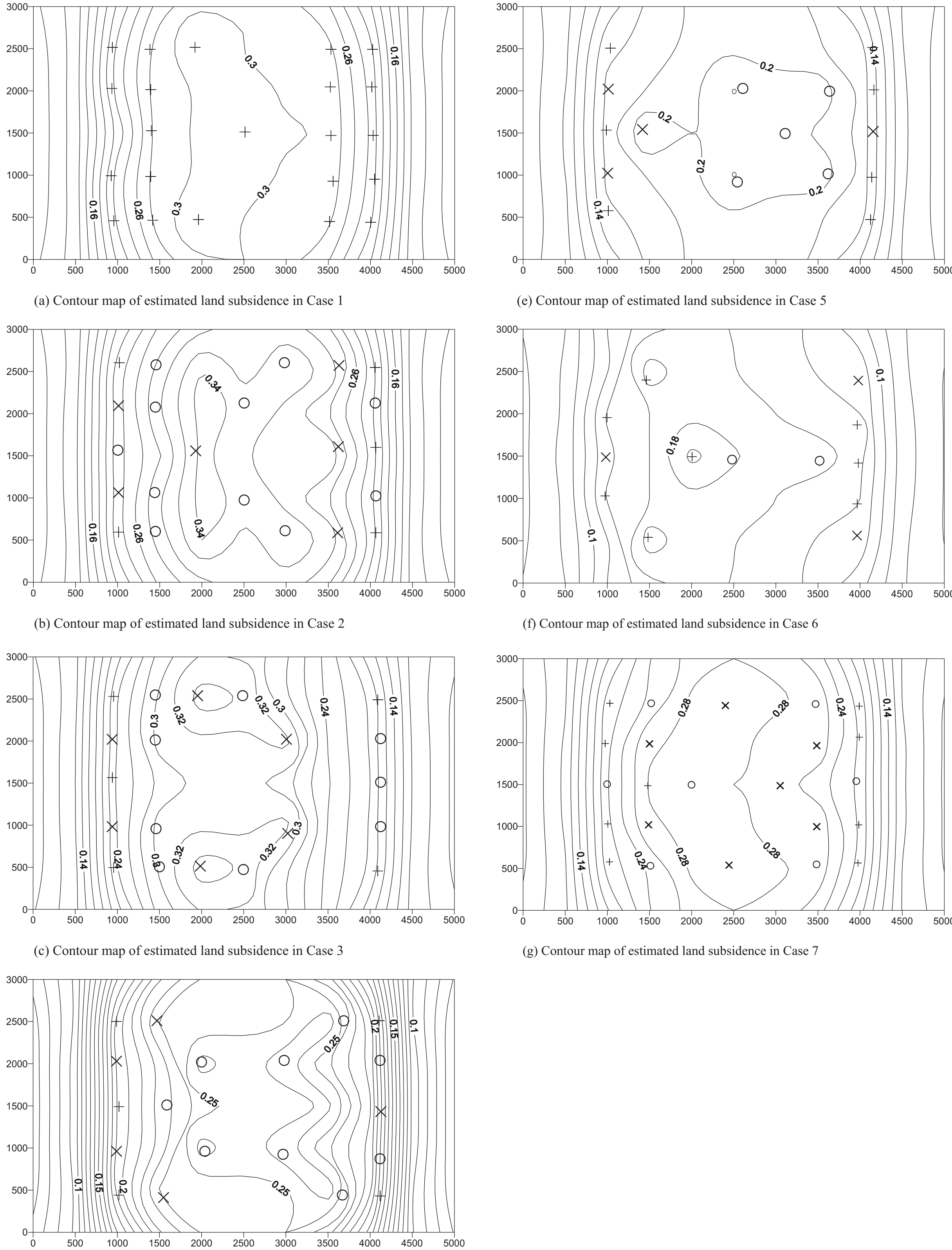

(a) Contour map of estimated land subsidence in Case 1

(b) Contour map of estimated land subsidence in Case 2

(c) Contour map of estimated land subsidence in Case 3

(d) Contour map of estimated land subsidence in Case 4

(e) Contour map of estimated land subsidence in Case 5

(f) Contour map of estimated land subsidence in Case 6

(g) Contour map of estimated land subsidence in Case 7

Fig. 6. Contour map of simulated subsidence in (a) Case 1; (b) Case 2; (c) Case 3; (d) Case 4; (e) Case 5; (f) Case 6; and (g) Case 7 where + represents well installation at the beginning of the first period; x represents well installation at the beginning of the second period; and ○ represents well installation at the beginning of the third period (unit: m)

Table 5. Optimal Pumping and Construction Policy between Different Demand Increasing Curves (Cases 2, 5, and 6)

Total water demand (10^6 m^3)	9.1								
Case number	Case 2			Case 5			Case 6		
Construction period number	I	II	III	I	II	III	I	II	III
Well numbers for each period	5	11	22	7	11	16	8	11	13
Present fixed cost value		280,392			239,127			218,494	
Present operation cost value		993,006			1,059,023			1,123,846	
Present total cost value		1,273,398			1,298,150			1,342,340	

Table 6. Optimal Pumping and Construction Policy for Different Land Subsidence Constraints (Cases 2 and 7)

Total water demand (10^6 m^3)	9.1					
Case number	Case 2			Case 7		
Construction period number	I	II	III	I	II	III
Well numbers for each period	5	11	22	9	16	23
Present fixed cost value		280,392			339,308	
Present operation cost value		993,006			991,979	
Present total cost value		1,273,398			1,331,287	

Acknowledgments

We would like to thank Dr. Hsiao, Dr. Tsai, the anonymous reviewers, editors, and helpers for their contributions to this study.

References

Adrian, O. G., Roudolph, D. L., and Cherry, J. A. (1999). "Analysis of long term land subsidence near Mexico City field investigation and predictive modeling." *Water Resour. Res.*, 35(11), 3327–3341.

Basagaoglu, H., and Yazicigil, H. (1994). "Optimal capacity-expansion planning in multiaquifer systems." *J. Water Resour. Plann. Manage.*, 120(6), 836–856.

Bayer, P., and Finkel, M. (2004). "Evolutionary algorithms for the optimization of advective control of contaminated aquifer zones." *Water Resour. Res.*, 40, W06506.

Bear, J., and Verruijt, A. (1987). *Modeling groundwater flow and pollution*, Reidel, Dordrecht, The Netherlands.

Biot, M. A. (1941). "General theory of three dimensional consolidation." *J. Appl. Phys.*, 12, 155–164.

Chang, L. C., Chen, Y. W., and Yeh, M. S. (2009). "Optimizing system capacity expansion schedules for groundwater supply." *Water Resour. Res.*, 45, W07407.

Chang, L. C., Chu, H. J., and Hsiao, C. T. (2007a). "Optimal planning of a dynamic pump-treat-inject groundwater remediation system." *J. Hydrol.*, 342(3–4), 295–304.

Chang, L. C., and Hsiao, C. T. (2002). "Dynamic optimal groundwater remediation including fixed and operation costs." *Ground Water*, 40(5), 481–490.

Chang, L. C., Shoemaker, C. A., and Liu, P. L. F. (1992). "Optimal time-varying pumping rates for groundwater remediation: Application of a constrained optimal control algorithm." *Water Resour. Res.*, 28(12), 3157–3173.

Chang, Y. L., Tsai, T. L., Yang, J. C., and Tung, Y. K. (2007b). "Stochastically optimal considering groundwater management land subsidence." *J. Water Resour. Plan. Manage.*, 133, 486–498.

Chen, C. X., Pei, S. P., and Jiao, J. J. (2003). "Land subsidence caused by groundwater exploitation in Suzhou City, China." *Hydrogeol. J.*, 11(2), 275–287.

Chu, H. J., and Chang, L. C. (2009). "Optimal control algorithm and neural network for dynamic groundwater management." *Hydrol. Process.*, 23, 2765–2773.

Chu, H. J., Hsiao, C. T., and Chang, L. C. (2005). "Optimal remediation design in groundwater systems by intelligent techniques." *Knowledge-Based Intelligent Information and Engineering Systems, Pt. 2, Proc.*, KES, Melbourne, 628–634.

Culver, T. B., and Shoemaker, C. A. (1992). "Dynamic optimal control for groundwater remediation with flexible management periods." *Water Resour. Res.*, 28(3), 629–641.

Culver, T. B., and Shoemaker, C. A. (1993). "Optimal control for groundwater remediation by differential dynamic programming with quasi-Newton approximations." *Water Resour. Res.*, 29(4), 823–831.

Don, N. C., et al. (2006). "Groundwater resources and management for paddy field irrigation and associated environmental problems in an alluvial coastal lowland plain." *Agric. Water Manage.*, 84(3), 295–304.

Goldberg, D. E. (1989). *Genetic algorithm in search, optimization, and machine learning*, Addison-Wesley, Reading, Mass.

Hsiao, C. T., and Chang, L. C. (2002). "Dynamic optimal groundwater management with inclusion of fixed costs." *J. Water Resour. Plann. Manage.*, 128(1), 57–65.

Hsiao, C. T., and Chang, L. C. (2005). "Optimizing remediation of an unconfined aquifer using a hybrid algorithm." *Ground Water*, 43, 904–915.

Huang, C., and Mayer, A. S. (1997). "Pump-and-treat optimization using well locations and pumping rates as decision variables." *Water Resour. Res.*, 33(5), 1001–1012.

Jacob, C. E. (1940). "On the flow of water in an elastic artesian aquifer." *Trans., Am. Geophys. Union*, 2, 574–586.

Jenkins, M. W., Lund, J. R., Howitt, R. E., Draper, A. J., Msangi, S. M., Tanaka, S. K., Ritzema, R. S., and Marques, G. F. (2004). "Optimization of California's water supply system: Results and insights." *J. Water Resour. Plann. Manage.*, 130(4), 271–280.

Jones, L., Willis, R., and Yeh, W. W. G. (1987). "Optimal control of nonlinear groundwater hydraulics using differential dynamic programming." *Water Resour. Res.*, 23(11), 2097–2106.

Larson, K. J., Basagaoglu, H., and Marino, M. A. (2001). "Prediction of optimal safe groundwater yield and land subsidence in the Los Banos-Kettleman City area, California, using a calibrated numerical simulation model." *J. Hydrol.*, 242, 79–102.

Liu, Y., and Helm, D. C. (2008). "Inverse procedure for calibrating parameters that control land subsidence caused by subsurface fluid withdrawal: 1. Methods." *Water Resour. Res.*, 44, W07423.

Mansfield, C. M., and Shoemaker, C. A. (1999). "Optimal remediation of unconfined aquifers: Numerical applications and derivative calculations." *Water Resour. Res.*, 35(5), 1455–1469.

Mansfield, C. M., Shoemaker, C. A., and Liao, L. Z. (1998). "Utilizing

Downloaded from ascelibrary.org by National Chiao Tung University on 04/24/14. Copyright ASCE. For personal use only; all rights reserved.

J. Hydrol. Eng. 2010.15:632-641.

sparsity in time-varying optimal control of aquifer cleanup." *J. Water Resour. Plan. Manage.*, 124(1), 15–21.

McKinney, D. C., and Lin, M. D. (1994). "Genetic algorithm solution of groundwater management models." *Water Resour. Res.*, 30(6), 1897–1906.

Morshed, J., and Kaluarachchi, J. J. (2000). "Enhancements to genetic algorithm for optimal groundwater management." *J. Hydrol. Eng.*, 5(1), 67–73.

Murray, D. M., and Yakowitz, S. J. (1979). "Constrained differential dynamic programming and its application to multireservoir control." *Water Resour. Res.*, 15(5), 1017–1027.

Ortega-Guerrero, A., Cherry, J. A., and Rudolph, D. L. (1993). "Large-scale aquitard consolidation near Mexico City." *Ground Water*, 31(5), 708–718.

Pulido-Velazquez, M., Andreu, J., and Sahuquillo, A. (2006). "Economic optimization of conjunctive use of surface water and groundwater at the basin scale." *J. Water Resour. Plan. Manage.*, 132(6), 454–467.

Sun, H., Grandstaff, D., and Shagam, R. (1999). "Land subsidence due to groundwater withdrawal: Potential damage of subsidence and sea level rise in southern New Jersey, USA." *Environ. Geol.*, 37(4), 290–296.

Verruijt, A. (1969). "Elastic storage of aquifers." *Flow through porous media*, R. J. M. de Wiest, ed., Academic, New York, 331–376.

Voivontas, D., Arampatzis, G., and Manoli, E. (2003). "Water supply modeling towards sustainable environmental management in small islands: The Case of Paros, Greece." *Desalination*, 156(1–3), 127–135.

Watkins, D. W., and McKinney, D. C. (1998). "Decomposition methods for water resources optimization models with fixed costs." *Adv. Water Resour.*, 21, 283–295.

Downloaded from ascelibrary.org by National Chiao Tung University on 04/24/14. Copyright ASCE. For personal use only; all rights reserved.

J. Hydrol. Eng. 2010.15:632-641.